

Assessing the corrosion protection of 8-hydroxyquinoline-cerium (III) complex for carbon steel in a NaCl solution

Anh Son Nguyen^{1,2,*}, Thuy Duong Nguyen^{1,2}, To Thi Xuan Hang^{1,2}, Thi Vy Anh
Vuong¹, Thu Thuy Pham¹, Thu Thuy Thai^{1,2}, Anh Truc Trinh^{1,2}, Nadine Pébère³

¹*Institute for Tropical Technology, Vietnam Academy of Science and Technology,
18 Hoang Quoc Viet, Cau Giay, Ha Noi, Viet Nam*

²*Graduate University of Science and Technology, Vietnam Academy of Science and Technology,
18 Hoang Quoc Viet, Cau Giay, Ha Noi, Viet Nam*

³*Université de Toulouse, CIRIMAT, UPS/INPT/CNRS, ENSIACET, 4, allée Emile Monso BP
44362, Toulouse 31432 Cedex 4, France*

*Email: nason@itt.vast.vn

Received: 10 November 2023; Accepted for publication: 3 February 2024

Abstract. In the present study, a complex between 8-hydroxyquinoline and cerium (III) (Ce-HQ) was synthesized in the presence of triethylamine. Afterwards, the complex was characterized by Field Emission Scanning Electron Microscopy (FESEM), Fourier-transform infrared spectroscopy (FTIR) and Thermo-Gravimetric Analysis (TGA). The inhibition efficiency of the Ce-HQ complex for the corrosion of carbon steel, evaluated by both Electrochemical Impedance Spectroscopy (EIS) and Potentiodynamic Polarization (PP) plots, reached 90 % after 2 h of immersion in a 0.01 M NaCl solution. Then, EIS measurements were carried out to evaluate the effect of the Ce-HQ complex, as inhibitive pigment, after incorporation in a waterborne epoxy coating applied over carbon steel plate. The total resistance (R_{total}) of the coated sample containing the Ce-HQ complex was higher ($3.6 \times 10^7 \Omega \text{ cm}^2$), after 35 days of exposure in a 0.5 M NaCl solution than the values obtained for the coating without Ce-HQ. The results showed that the EP/Ce-HQ coating provided not only corrosion protection by the Ce (III) ions and 8HQ release at the metal/coating interface, but also improved the barrier properties. This work proposed a new type of inhibitive pigments which can be used to develop effective coatings for corrosion protection.

Keywords: 8-Hydroxyquinoline Complex, corrosion inhibitor, electrochemical impedance spectroscopy, cerium (III) ions.

Classification numbers: 2.10.2, 2.5.3, 2.3.1.

1. INTRODUCTION

Carbon steel has been widely used in various industries; however, corrosion generates severe degradation of materials, which has serious and significant repercussions. Thus, corrosion protection of metals and alloys remains challenging [1, 2]. Recently, many efforts have been made to prevent corrosion and deterioration of metallic structures in transportation systems, buildings, and other related areas, to curb economic losses [3, 4]. Among the most efficient methods to prevent carbon steel corrosion, organic coatings have held great significance owing to their effective ability to act as barriers to impede aggressive species to reach the metallic substrate. Moreover, the corrosion protection performance of organic coatings can be enhanced by incorporating inorganic, organic, or inorganic/organic hybrid inhibitive pigments [5 - 8].

Conventional corrosion inhibitors used for carbon steel include inorganic salts and organic compounds. Organic compounds typically act as effective corrosion inhibitors by adsorbing on the metals surface due to the creation of coordination bonds between sulfur (S), oxygen (O), nitrogen (N) atoms and the metal surface, facilitated by the availability of lone electron pairs or π bonds [9-11]. Among organic inhibitors, 8-hydroxyquinoline (8-HQ) is recognized for its chelating abilities on carbon steel surface, thanks to its functional groups: aromatic ring, hydroxyl (OH) and $-N=C-$ bond [6, 12, 13]. During the inhibition process, complexes are formed between dissolved cations (Fe^{2+} or Fe^{3+}) present on the surface and 8-HQ. These complexes establish a protective barrier that effectively hinders further dissolution [12, 13].

On the other hand, rare earth salts, and in particular cerium salts are known to be “green” inorganic inhibitors, which have the capacity to protect carbon steel [14-17]. During exposure to corrosive environments, the presence of Ce (III) cations gradually leads to the formation of Ce (III/IV) oxide/hydroxides protective layer on cathodic regions [15]. However, some inorganic cerium salts readily dissolve in water, potentially resulting in negative influence when they are incorporated into organic coatings.

The synthesis of “green” inhibitors, exhibiting strong corrosion inhibition properties on carbon steel as well as having limited water solubility and appropriate release rate from coatings, has received great attention in the last decades. Addressing these challenges, cerium cations can interact with organic groups, resulting in the formation of inorganic-organic salts or complexes that exhibit reduced solubility [18 - 20]. In addition, the inorganic-organic salts or complexes can act as mixed corrosion inhibitor for carbon steel, creating protective oxide/hydroxides layer on the cathodic sites and chemical adsorption of organic molecules on the anodic sites [14, 21, 22]. Moreover, the binding of organic ligands with Ce cations through chelation can lead to the formation of high molecular weight complexes, which results in the physical adsorption onto the substrate [22].

In the present work, cerium (III) complex of 8-hydroxyquinoline (Ce-HQ complex) was synthesized and characterized using Field Emission Scanning Electron Microscopy (FESEM), Fourier-Transform Infrared Spectroscopy (FTIR) and Thermo-Gravimetric Analysis (TGA). The inhibition efficiency of the Ce-HQ complex was evaluated by using electrochemical methods such as, Electrochemical Impedance Spectroscopy (EIS) and polarization curves, first in a neutral aqueous solution on bare carbon steel and then, after incorporation in a waterborne epoxy coating deposited onto carbon steel plate. In both cases, the protection afforded by the Ce-HQ was compared to that obtained with the Ce salts ($Ce(NO_3)_3$) or the 8HQ.

2. MATERIALS AND METHODS

2.1. Materials

A two-component water-based coating was used: a polyaminoamide (Epikure 8537-WY-60, Momentive) as hardener and a bisphenol epoxy polymer (Epikote 828, Hexion) as base. Cerium (III) nitrate hexahydrate ($\text{Ce}(\text{NO}_3)_3 \cdot 6\text{H}_2\text{O}$), 8-hydroxyquinoline (8HQ) and triethylamine (Et_3N) used to synthesize the 8-Hydroxyquinoline Complex with Cerium (III) (Ce-HQ) were purchased from Merck. The organic coating was deposited on carbon steel plates (150 mm \times 100 mm \times 1 mm). Before coating application, the steel was polished with SiC paper (grade 400) then cleaned with distilled water and ethanol. The electrolyte was a 0.5 M solution of NaCl (reagent grade) in contact with air.

For the electrochemical in solution, the working electrode was a rotating disk consisting of a carbon steel rod of 1 cm² cross-sectional area. A thermo-retractable sheath prevented the cylindrical area from making contact with the solution; the electrode surface was only the cross-section. The sample selected for the study was an XC35 carbon steel and had the following composition in wt. %: C = 0.35, Mn = 0.65, Si = 0.25, P = 0.035, S = 0.035 and Fe to 100. For all the experiments, the samples were polished with SiC paper (from grade 240 to grade 1200), cleaned in water and then dried in warm air. The electrolyte was a 0.01 M solution of NaCl (reagent grade) in contact with air.

2.2. Synthesis of Ce-HQ complex

The synthesis of Ce-HQ process is schematically described in Figure 1. Cerium (III) salt (2.2 g) was first dissolved in 100 ml distilled water, while 8HQ (2.2 g) and triethylamine (2.1 ml) were mixed in 100 ml ethanol/water (v/v, 50/50). Afterwards, the 8HQ/ Et_3N mixture was put into a reflux condenser and the temperature was increased up to 60 °C. Then, the $\text{Ce}(\text{NO}_3)_3$ solution was added drop-wise. The reaction took place at 60 °C within 4 h under vigorously stirring. The obtained precipitate was filtered and washed several times with distilled water to remove the soluble compounds. The collected product was then dried at 70 °C within 24 h.

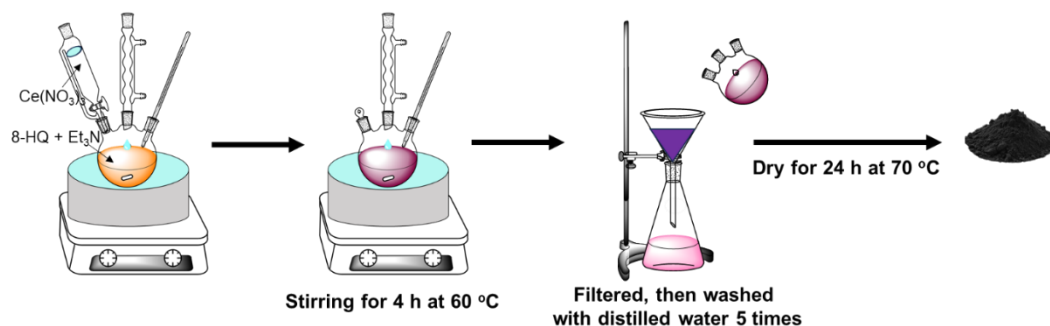


Figure 1. Schematic illustration of the synthesis of the Ce-HQ complex.

2.3. Preparation of the waterborne epoxy coatings

Four different coating systems were prepared to compare the effect of $\text{Ce}(\text{NO}_3)_3$, 8HQ or Ce-8HQ. First, the compounds were dissolved and dispersed in ethanol/water (70/30) by magnetic stirring, combined with ultrasonic probe technique, for 30 min. Then, the solutions were incorporated into the waterborne epoxy system with a concentration of 1 wt.%.

The mixtures were vigorously stirred for 1 h before the application onto the carbon steel plates. The prepared coatings were applied by spin-coating (400 rpm for 10 s) and dried at room temperature for one week. The film thickness was determined at about 28 ± 2 μm via a Minitest

600 Erichen digital meter. The epoxy coating with $\text{Ce}(\text{NO}_3)_3$, 8HQ, Ce-HQ and without inhibitors are denoted EP/Ce, EP/HQ, EP/Ce-HQ and EP, respectively.

2.4. Methods

The morphology of the Ce-HQ complex particles and the compatibility of the pigments with the epoxy matrix were characterized by FESEM (Hitachi S-4800) on the cross-section of the samples. FTIR spectra of 8HQ and Ce-HQ were obtained on a Nexus 670 Nicolet spectrometer with a resolution of 8 cm^{-1} using transmittance mode with KBr. The spectra were obtained in the region of $400 - 4000\text{ cm}^{-1}$. TGA was carried out with a Netzsch TG 209F1 Libra under N_2 conditions. The temperature range was from room temperature to $800\text{ }^\circ\text{C}$ with $10\text{ }^\circ\text{C}/\text{min}$.

Electrochemical measurements (EIS and polarization curves) were carried out with a Biologic VSP300 apparatus. A classical three-electrode cell was used, in which the carbon steel rod was the working electrode, a saturated calomel electrode (SCE) and a platinum grid were used as reference and counter electrodes, respectively. The impedance diagrams were obtained at the open circuit potential, under potentiostatic condition, with 10 mV peak-to-peak sinusoidal voltage, over a frequency range of 100 kHz to 1 Hz with 8 points per decade (first up to 90 min) and to 10 mHz (after 2 h of immersion). Then, the anodic and cathodic polarization curves were recorded at a scan rate of $1\text{ mV}/\text{s}$. The impedance diagrams for the coated samples were acquired with the same parameters as those used for the carbon steel rod in the solution, except the amplitude which was 30 mV peak-to-peak. For the electrochemical experiments, measurements were performed three times to ensure reproducibility.

3. RESULTS AND DISCUSSION

3.1. Characterization of Ce-HQ complex

The morphology of Ce-HQ complex was characterized by FESEM images. Figure 2a shows that the Ce-HQ particle displays a typical rectangular-like structure with a size around $5 - 10\text{ }\mu\text{m}$. It seems that this complex was developed by the combination of multi-nanosheets with a thickness of $100 - 200\text{ nm}$ (Figure 2b).

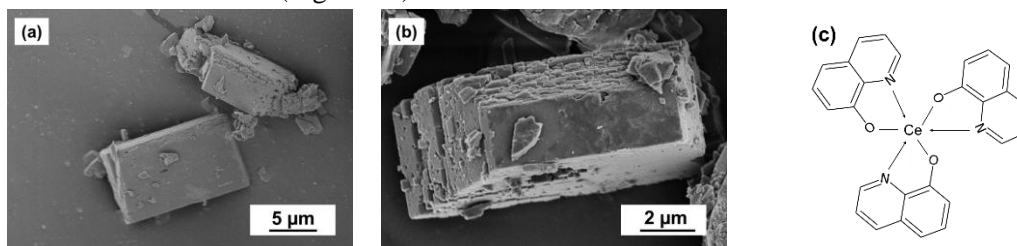


Figure 2. SEM micrographs of the Ce-HQ particles: (a) Magnification $\times 3\ 500$ et (b) Magnification $\times 10\ 000$. (c) Structure of the Ce-HQ complex based on reference [23].

That phenomenon can be explained by the chemical structure of the complex, as shown in Figure 2c by analogy with the work of El-Wahab [23]. According to this work, one cerium atom can react with three 8HQ through the formation of $\text{C} - \text{O}$ and $\text{C} \leftarrow \text{N}$ bonds, where oxygen and nitrogen of 8HQ are donor atoms. The synthesized Ce-HQ complex was analyzed by FTIR spectroscopy (Figure 3a). The Ce-HQ complex spectrum reveals the characteristic bands of 8HQ. The adsorption band at 1568 cm^{-1} corresponds to the stretching of the $\text{C}=\text{C}$ bond of the

quinoline ring [20]. Besides, due to the reaction between Ce (III) ions and 8HQ, the characteristic bands of the C=N, C-N and C-O bond were slightly shifted to 1495 cm^{-1} , 1274 cm^{-1} and 1105 cm^{-1} , respectively. The bands observed for the 8HQ appear at 1502 cm^{-1} , 1288 cm^{-1} and 1094 cm^{-1} [6, 24]. The absorption band at 484 cm^{-1} is assigned to the stretching vibration of O coordinated to cerium (III) ions [20]. The FTIR analysis results illustrated the complex formation of 8HQ with cerium (III) ions.

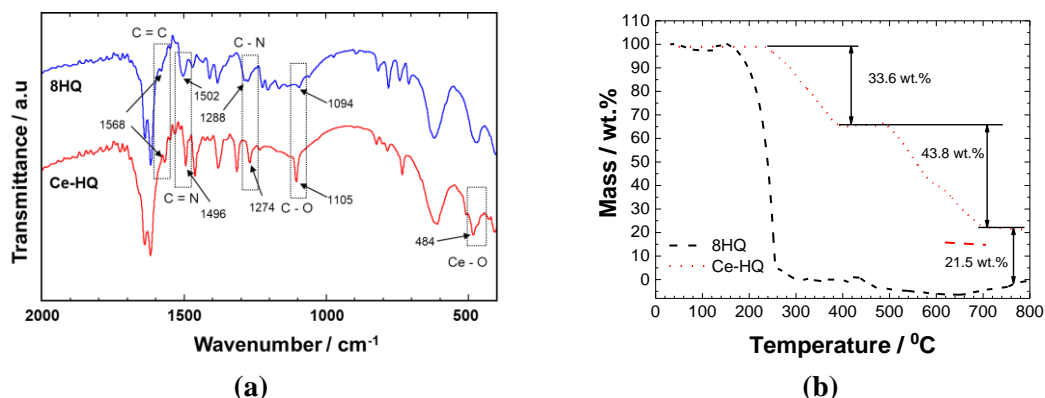


Figure 3. FTIR spectra of the 8HQ and the Ce-HQ complex (a); and Thermograms of the 8HQ and the Ce-HQ complex (b).

The formation of Ce-HQ complex can also be confirmed from the thermal properties by using TGA technique. Figure 3b shows that the degradation of 8HQ occurs around $170\text{ }^{\circ}\text{C}$, while that of Ce-HQ is shifted to higher temperatures with two temperature ranges: $235\text{ }^{\circ}\text{C} - 390\text{ }^{\circ}\text{C}$ and $480\text{ }^{\circ}\text{C} - 700\text{ }^{\circ}\text{C}$. Due to the rectangular-like structure of the synthesized complex and to the thickness of the particles, the particle surface was first decomposed corresponding to the first mass loss in the TGA curve. Then, the thermal degradation continues with all the organic part in the inorganic-organic complex structure. The overall mass loss at the end of the TGA test is about 77.4 % in agreement with the value calculated from the chemical structure (Figure 2c) which is 75.5 %. This behaviour might be explained by the presence of 8HQ adsorbed on the surface of the complex particles.

3.2. Inhibitor efficiency of Ce-HQ complex in NaCl solution

Impedance measurements and polarization curves were carried out to assess the efficiency of the Ce-HQ complex for the corrosion protection of the carbon steel. The electrochemical results were obtained in the presence of $\text{Ce}(\text{NO}_3)_3$, 8HQ and Ce-HQ at a concentration of 1 g/L, for comparison.

First, the variation of the corrosion potential, E_{corr} , versus the exposure time in a 0.01 M NaCl solution with and without inhibitors was studied. Figure 4 shows that, at the beginning of immersion, the E_{corr} values obtained in the solution containing 8HQ and Ce-HQ are around -0.47 V and -0.49 V , respectively, whereas the E_{corr} values are about -0.37 V and -0.38 V in the solution containing $\text{Ce}(\text{NO}_3)_3$ and without inhibitors. This potential difference might be attributed to the cathodic inhibition effect of 8HQ on the carbon steel. When the immersion time increases, the E_{corr} value obtained in the solution with Ce-HQ shifts to the E_{corr} value obtained with cerium salt, indicating that the Ce (III) ions were released from the hybrid complex. Then, the E_{corr} values of the carbon steel immersed in the solution containing $\text{Ce}(\text{NO}_3)_3$ and Ce-HQ complex are almost similar.

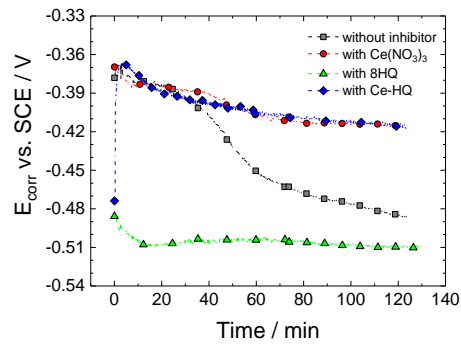


Figure 4. Corrosion potential (E_{corr}) for the carbon steel electrode as a function of exposure time in a 0.01 M NaCl solution with and without inhibitors (indicated in the figure).

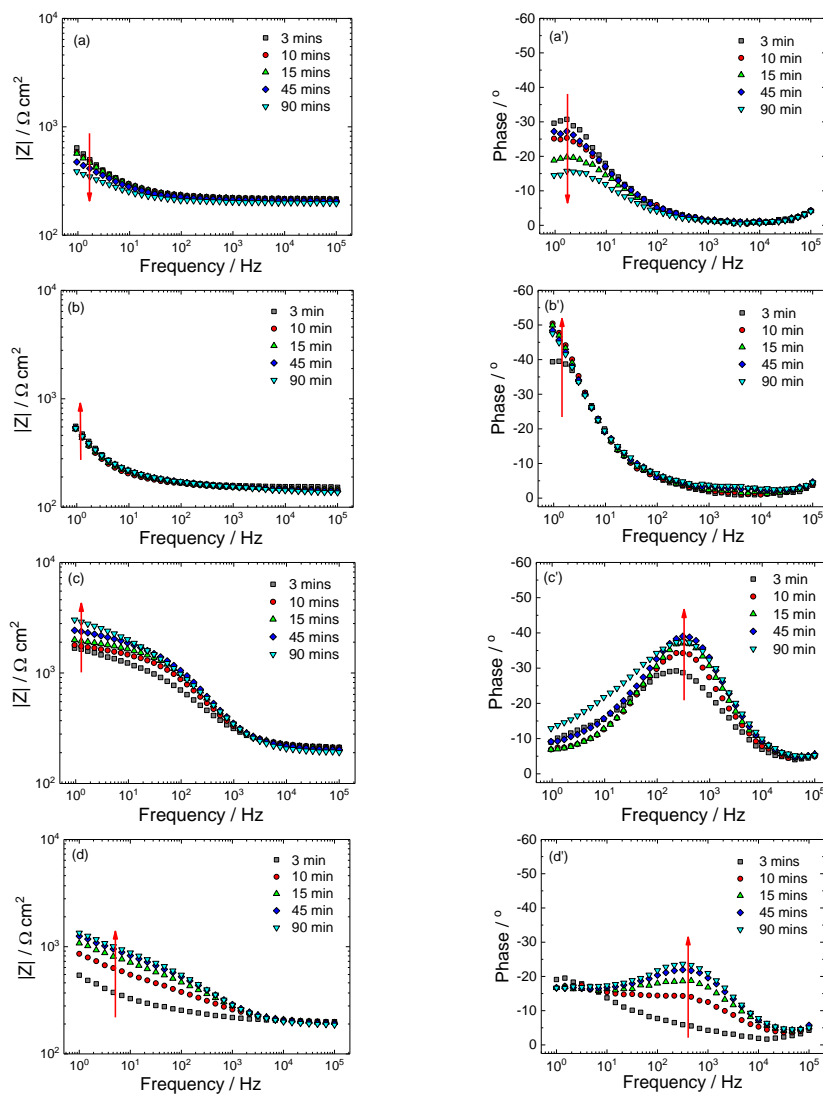


Figure 5. EIS diagrams obtained at E_{corr} during the first exposure time (up to 90 min) for the carbon steel electrode in a 0.01 M NaCl without inhibitor (a, a') and with $\text{Ce}(\text{NO}_3)_3$ (b, b'), 8HQ (c, c') and Ce-HQ (d, d').

The impedance diagrams of the carbon steel obtained for the first 90 min of immersion in the 0.01 M NaCl solution with and without inhibitors are shown in Figure 5. Without inhibitor, the impedance modulus at low frequency decreases when the immersion times increases. In the presence of the inhibitors, the impedance modulus at low frequency increases for increasing immersion time. This could be explained by the progressive formation of a protective layer onto the carbon steel surface or by the decrease of the active surface area due to the inhibitors adsorption. However, the shape of the impedance diagrams is different which would be indicative of different inhibition mechanisms. For the solution containing cerium salt, the Ce (III) ions would rapidly react on the cathodic sites on the carbon steel surface [15]. The fast interaction of the Ce salt with the surface is shown by the rapid stabilization of the impedance diagrams after 10 min of immersion. In the case of 8HQ, it may be assumed the progressive formation of insoluble chelates between the Fe^{2+} ions (anodic reaction) and the 8HQ on the carbon steel surface [6, 12]. This hypothesis is consistent with both the increase of the impedance modulus, from $1700 \Omega \text{ cm}^2$ to $3000 \Omega \text{ cm}^2$ between 3 min and 90 min of immersion and the presence of a time constant between 10^2 Hz - 10^3 Hz . For the Ce-8HQ containing solution, it can be observed a time constant which progressively appears in the frequency domain 10^2 Hz - 10^3 Hz . This observation suggests the formation of the chelate between the Fe^{2+} ions and the 8HQ, as already discussed but the inhibition effect of Ce (III) for the short immersion time seems negligible. These results could be explained by the fact that the Ce-HQ complex is going to release more 8HQ than Ce (III) ions in the aqueous electrolyte. Thus, in the first 90 min the chelates formation would be significant, but despite this, the metal substrate is still protected with rather high impedance value. The impedance modulus at low frequency reaches $1350 \Omega \text{ cm}^2$ after 90 min of immersion.

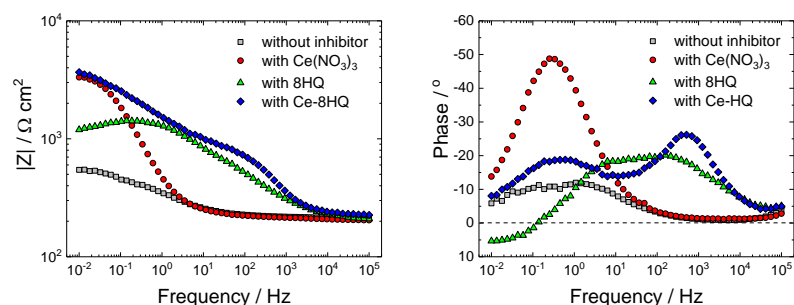


Figure 6. EIS diagrams for the carbon steel electrode obtained at E_{corr} after 2 h of immersion time in a 0.01 M NaCl with and without inhibitors (indicated in the figure).

Figure 6 shows the impedance diagrams obtained after 2 h of exposure to the NaCl solution with and without inhibitors. The comparison of the impedance diagrams emphasises the combined effect of the 8HQ and the Ce salts when the Ce-HQ complex is introduced in the solution. For the electrode immersed in the solution containing the Ce-HQ complex, two-time constants are observed, one at 1 Hz and one at 1 kHz, which would correspond to the oxide/hydroxide Ce (III/IV) formation and to the chelate/8HQ layer, respectively. Due to the combination of two inhibitive effects on the surface, the impedance modulus at 10 mHz for $Ce(NO_3)_3$ and Ce-8HQ complex had a similar value of, about $3500 \Omega \text{ cm}^2$, even though the phase angle at 1 Hz for $Ce(NO_3)_3$ is greater than that for Ce-HQ complex, -50 degrees compared to -18 degrees, respectively. In the presence of 8HQ, the impedance decreases at low frequency. The impedance modulus is lower than those obtained with the other inhibitors, $|Z|_{10 \text{ mHz}} = 1200 \Omega \text{ cm}^2$. This result could be linked to the solubility of the Fe/8HQ chelate. A high solubility of the

chelate would lead to the corrosion acceleration. From the EIS data, the inhibitors efficiency (IE) is calculated with the following formula:

$$IE (\%) = \left(\frac{R_p^i - R_p^0}{R_p^i} \right) \times 100\%$$

where, R_p^i and R_p^0 are the polarisation resistance values obtained for the carbon steel immersed in the NaCl solution with and without inhibitors, respectively. These values were extracted graphically from the impedance diagrams by using the impedance modulus at low frequency. The values are reported in Table 1. The IE for the $Ce(NO_3)_3$ and the Ce-HQ are higher (89 - 90 %) than for the 8HQ (65 %).

Table 1. Inhibitor efficiency (IE) calculated from the EIS data and from the polarization curves for the carbon steel electrode after 2 h of exposure in the 0.01 M NaCl with and without inhibitors.

Samples	R_p ($\Omega \text{ cm}^2$)	I_{corr} ($\mu\text{A cm}^{-2}$)	E_{corr} (V)	IE (%) from EIS data	IE (%) from polarization curves
Without inhibitor	336	252	-0.50	-	-
$Ce(NO_3)_3$	3096	23	-0.42	89	91
8HQ	973	112	-0.54	65	56
Ce-HQ	3433	24	-0.44	90	90

Inhibition mechanisms can be also investigated by the polarization curves. Figure 7 compares the cathodic and anodic curves obtained for carbon steel after 2 h of immersion in a 0.01 M NaCl containing the different inhibitors. It shows that the corrosion potential (E_{corr}) value for 8HQ shifted toward the negative direction ($E_{\text{corr}} = -0.54 \text{ V}$), however the E_{corr} for cerium salt and Ce-HQ compounds was displaced in reversed direction ($E_{\text{corr}} = -0.42 \text{ V}$ and -0.44 V , respectively), compares to E_{corr} obtained in the solution without inhibitor ($E_{\text{corr}} = -0.50 \text{ V}$).

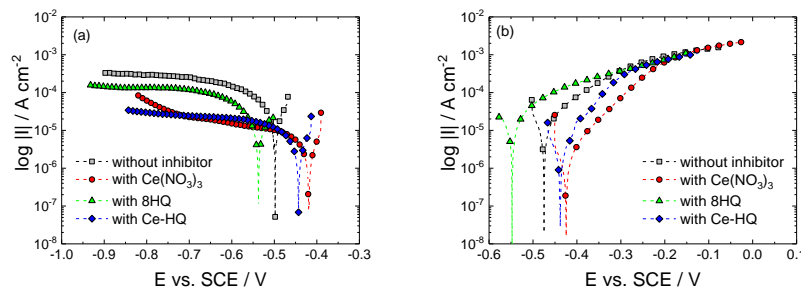


Figure 7. Polarization curves obtained for the carbon steel after 2 h of exposure in a 0.01 M NaCl with and without inhibitors (indicated in the figure): (a) cathodic part and (b) anodic part.

The polarization curves clearly illustrate the inhibition effect through the corrosion current density, which allows the inhibition efficiency to be calculated by the following equation:

$$IE (\%) = \left(\frac{i_{\text{corr}}^o - i_{\text{corr}}^i}{i_{\text{corr}}^o} \right) \times 100\%$$

where, i_{corr}^i and i_{corr}^o are the corrosion current densities values obtained for the carbon steel immersed in the NaCl solution with and without inhibitors, respectively. These values are reported in Table 1 and compared to those obtained from the impedance data. The corrosion current density obtained for the carbon steel without inhibitor is about $250 \mu\text{A/cm}^2$. The values

obtained for $\text{Ce}(\text{NO}_3)_3$ and Ce-HQ are almost identical, 23 - 24 $\mu\text{A}/\text{cm}^2$. Therefore, the inhibitive efficiencies of the cerium salt and of the inorganic-organic complex are rather similar (90 - 91 %) and higher than that of 8HQ (56 %). The inhibitive efficiencies calculated from the polarisation curves and from the EIS data are in good agreement. It can be seen that the anodic current densities are higher in the presence of 8HQ compared to those measured without inhibitor (Figure 7 b). This result might be attributed to an acceleration of the iron dissolution due to the formation of soluble chelates with the 8HQ, has already discussed.

3.3. Evaluation of the anticorrosion properties of epoxy coatings

The morphology of the inhibitors in the epoxy coating was observed by FESEM. Figure 8 reveals a good compatibility between the inhibitors and the epoxy. For the coating with $\text{Ce}(\text{NO}_3)_3$, it was clearly observed that the cerium salt crystals tend to agglomerate in the organic matrix. Moreover, due to a poor compatibility between inorganic and organic compounds, some voids are detected at the salt/epoxy matrix interface. This behaviour might introduce pathway for fast penetration of the electrolyte into the coating. In contrast, the 8HQ particles are not detected in the FESEM cross-section micrograph that can improve the barrier properties of the coating. In the FESEM image of the epoxy containing Ce-HQ complex, the rectangular shape of the particles can be visualised in the epoxy matrix. However, there is no obvious space gaps around them.

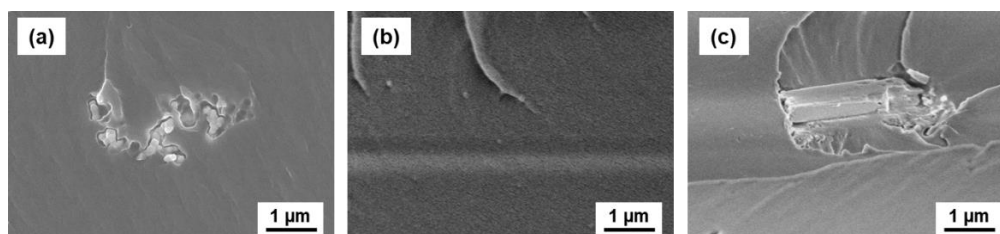


Figure 8. FESEM cross-sectional images of the waterborne epoxy containing: (a) with $\text{Ce}(\text{NO}_3)_3$, (b) with 8HQ and (c) with Ce-HQ complex.

The impedance of the coated samples with and without inhibitors was measured after various immersion times, up to 35 days, in a 0.5 M NaCl solution (Figure 9). After one day of exposure, all samples presented a single time-constant attributed to the coatings resistance (Figure 9a). The solubility and the compatibility of the additives can directly affect the barrier properties of the epoxy coating. The epoxy coating containing $\text{Ce}(\text{NO}_3)_3$ (soluble in the NaCl solution) has the lower impedance value ($|Z|_{1\text{ Hz}} = 8.0 \times 10^6 \Omega \text{ cm}^2$), meanwhile, the coating with the Ce-HQ complex (little soluble) and with the 8HQ (compatible with the epoxy matrix) are characterized by slightly lower impedance values compared to the coating without inhibitor, $|Z|_{1\text{ Hz}}$ decreased from $1.7 \times 10^6 \Omega \text{ cm}^2$ to $1.4 \times 10^6 \Omega \text{ cm}^2$. After 7 days of exposure (Figure 9b), the impedance diagram for the EP/Ce-HQ reveals two-time constant attributed the protective film formed by the organic-inorganic complex and the epoxy coating. With the multi protective layers, the impedance of EP/Ce-HQ has the highest value, $6.4 \times 10^7 \Omega \text{ cm}^2$, compared to $3.1 \times 10^7 \Omega \text{ cm}^2$, $3.0 \times 10^7 \Omega \text{ cm}^2$ and $1.4 \times 10^7 \Omega \text{ cm}^2$, corresponding to EP/HQ, EP and EP/Ce. At the end of the test, 35 days of immersion, the impedance value obtained for the EP/Ce-HQ coating is always the highest, while the EP/HQ coating exhibits a higher restriction of the diffusion of the corrosive species to the metallic substrate than the pristine epoxy coating (Figure 9c). It shows that the presence of 8HQ provides not only compatible with epoxy matrix, but also improving the barrier properties of the epoxy system. This result was demonstrated by Balaskas *et al.* [25].

The total resistance of the coated samples (combination of the coating resistance and charge transfer resistance), R_{total} , was graphically determined by extrapolation the EIS data at low

frequency. The variation of R_{total} as a function of the immersion time for the different coatings is shown Figure 10.

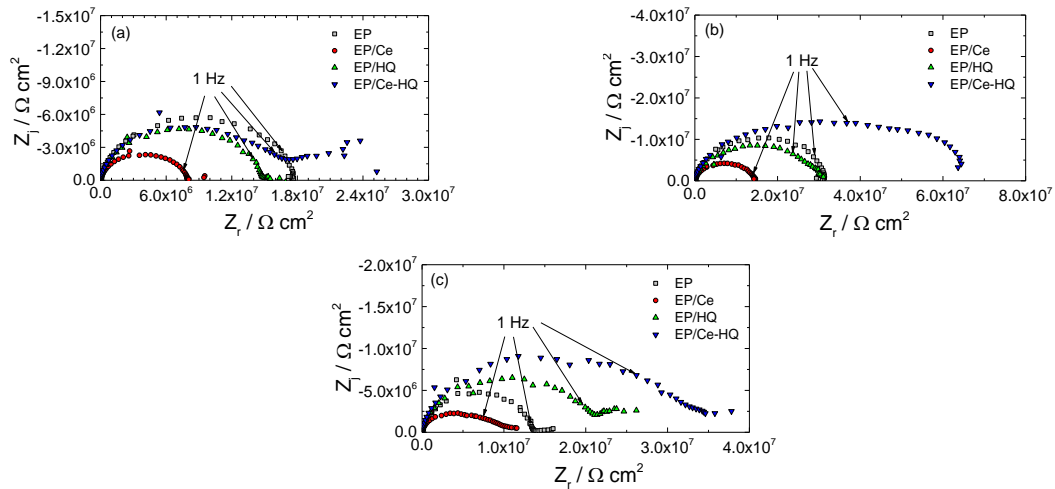


Figure 9. Impedance diagrams (Nyquist plot) obtained at E_{corr} after: 1 day (a), 7 days (b) and 35 days (c) of immersion time in a 0.5 M NaCl solution for the waterborne epoxy coating, both with and without inhibitor, deposited onto carbon steel substrate.

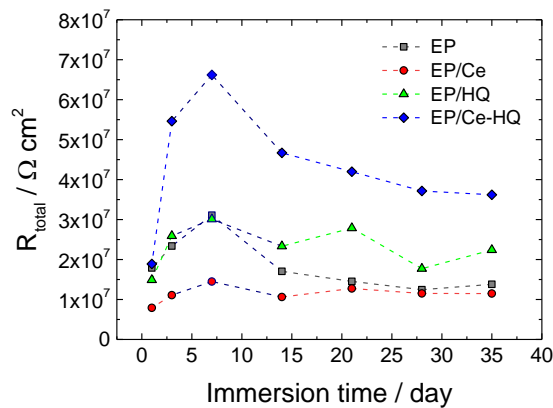


Figure 10. Variation of R_{total} values graphically determined from EIS data obtained on the waterborne epoxy coatings, with and without inhibitors, deposited onto carbon steel substrate.

It is noticed that, during the first immersion days, the value of R_{total} for all the samples increased even through the coatings were exposed into the corrosive solution. This unexpected behaviour has been already observed in the case of waterborne systems and attributed to a complementary process resulting of the coalescence of the polymer particles activated by the water uptake [26 - 28]. This contributes to increase the barrier properties of the coatings and the impedance values increased. The EP/Ce-HQ coatings, with the mix of the formation of protective layer by Ce-HQ complex released and the reticular epoxy matrix by the water penetration, shows a raise more significantly of R_{total} value than the other coatings, $6.6 \times 10^7 \Omega \text{ cm}^2$. After 7 days of exposure in 0.5 M NaCl solution, the R_{total} of all samples rapidly diminished, but the R_{total} of EP/Ce-HQ had still reached the highest value at the end of test, $3.62 \times 10^7 \Omega \text{ cm}^2$. With the presence of 8HQ, the EP/HQ coating also shows a better performance than that of pristine epoxy, $2.2 \times 10^7 \Omega \text{ cm}^2$ and $1.38 \times 10^7 \Omega \text{ cm}^2$, respectively. For the EP/Ce coating, although the R_{total} obtained was the lowest value, but it seems that value of EP/Ce coatings is the most stable over the time, from $7.9 \times 10^7 \Omega \text{ cm}^2$ to $1.1 \times 10^7 \Omega \text{ cm}^2$. The low R_{total}

can be explained by the release of the $\text{Ce}(\text{NO}_3)_3$ from the coating, that introduces voids in the coating facilitating the penetration of the aggressive species throughout the coating. On the other hand, the Ce (III) ions could rapidly establish a protective oxide/hydroxide layer (as demonstrated above) at the metal/coating interface, preventing the corrosion process.

4. CONCLUSIONS

In the present work, the Ce-HQ inorganic-organic complex was synthesized and its efficiency was determined from EIS and polarization curves in the 0.01 M NaCl solution. The results showed that the complex played a role which combines the inhibitive action of Ce salts and 8HQ. The protection afforded by the Ce-HQ complex was progressively enhanced as a function of the exposure time. A good inhibition efficiency, about 90 % (similar to Ce (III) and better than 8HQ), was measured after 2 h of immersion time. Good agreement between EIS data and the polarization curves was observed.

When incorporated into the waterborne epoxy system, the Ce-HQ complex displayed a good compatibility with the organic matrix. From EIS data, it was concluded that the highest protection was obtained in the presence of Ce-HQ introduced in the coating due to the presence of both Ce (III) and 8HQ inhibitors. The first one prevented corrosion phenomena at the metal/coating interface, while the second helped to improve the barrier properties of epoxy system. With these positive results, Ce-HQ complex is a potential candidate for non/less-toxic inhibitive pigments. As a next step, both the coating formulation and inhibitors content should be modified to optimize the coating performance. It is noteworthy that Viet Nam has good sources of Ce which is a great advantage for further research using cerium compounds as inhibitive species in protective coatings.

Acknowledgements. The authors gratefully acknowledge the financial support of Vietnam Academy of Science and Technology under Grant QTFR01.02/20-21. This study was also prepared in the collaboration between France and Viet Nam under the associated international laboratory project “Functional Composite Materials (FOCOMAT)”.

CRedit authorship contribution statement. Anh Son Nguyen: Investigation, Formal analysis, Writing. Thuy Duong Nguyen: Formal analysis. To Thi Xuan Hang: Methodology. Formal analysis. Thi Vy Anh Vuong: Preparation sample. Thu Thuy Pham: Investigation, Writing. Thu Thuy Thai: Formal analysis. Anh Truc Trinh: Formal analysis. Nadine Pébère: Methodology, Formal analysis, Writing.

Declaration of competing interest. The authors declare that they have no known competing financial interests or personal relationships that could have appeared to influence the work reported in this paper.

REFERENCES

1. Dwivedi D., Lepková K., Becker T. - Carbon steel corrosion: a review of key surface properties and characterization methods, *RSC Advances* **7** (2017) 4580-4610. <https://doi.org/10.1039/C6RA25094G>
2. Aslam R., Mobin M., Zehra S., Aslam J. - A comprehensive review of corrosion inhibitors employed to mitigate stainless steel corrosion in different environments, *J. Mol. Liq.* **364** (2022) 119992. <https://doi.org/10.1016/j.molliq.2022.119992>
3. Hang T. T. X., Dung N. T., Truc T. A., Duong N. T., Truoc B. V., Vu P. G., Hoang T., Thanh D. T. M., Olivier M. G. - Effect of silane modified nano ZnO on UV degradation of polyurethane coatings. *Prog. Org. Coat.* **79** (2015) 68-74. <https://doi.org/10.1016/j.porgcoat.2014.11.008>

4. Brenna A., Beretta S., Ormellese M. - AC Corrosion of Carbon Steel under Cathodic Protection Condition: Assessment, Criteria and Mechanism, *A Review Materials* **13** (9) (2020) 2158. <https://doi.org/10.3390/ma13092158>
5. Hang T. T. X., Truc T. A., Duong N. T., Pébère N., Olivier M. G. - Layered double hydroxides as containers of inhibitors in organic coatings for corrosion protection of carbon steel, *Prog. Org. Coat.* **74** (2012) 343-348. <https://doi.org/10.1016/j.porgcoat.2011.10.020>
6. Truc T. A., Thuy T. T., Oanh V. K., Hang T. T. X., Nguyen A. S., Caussé N., Pébère N. - 8-hydroxyquinoline-modified clay incorporated in an epoxy coating for the corrosion protection of carbon steel, *Surf. Interfaces* **14** (2019) 26-33. <https://doi.org/10.1016/j.surfin.2018.10.007>
7. Salazar-Bravo P., Del Ángel-López D., Torres-Huerta A.M., Domínguez-Crespo M.A., Palma-Ramírez D., López-Oyama A.B. - Corrosion investigation of new hybrid organic/inorganic coatings for carbon steel substrates: Electrochemical and surface characterizations. *Prog. Org. Coat.* **135** (2019) 51-64. <https://doi.org/10.1016/j.porgcoat.2019.05.038>
8. Pepe A., Galliano P., Aparicio M., Durán A., Ceré S. - Sol-gel coatings on carbon steel: Electrochemical evaluation, *Surf. Coat. Technol.* **200** (2006) 3486-3491. <https://doi.org/10.1016/j.surfcoat.2005.07.102>
9. Thoume A., Elmakssoudi A., Left D.B., Benzbiria N., Benhiba F., Dakir M., Zahouily M., Zarrouk A., Azzi M., Zertoubi M. - Amino acid structure analog as a corrosion inhibitor of carbon steel in 0.5 M H₂SO₄: Electrochemical, synergistic effect and theoretical studies, *Chem. Data Collect.* **30** (2020) 100586. <https://doi.org/10.1016/j.cdc.2020.100586>
10. Badr G. E. - The role of some thiosemicarbazide derivatives as corrosion inhibitors for C-steel in acidic media, *Corros. Sci.* **51** (2009) 2529-2536. <https://doi.org/10.1016/j.corsci.2009.06.017>
11. Chauhan D. S., Ansari K. R., Sorour A. A., Quraishi M. A., Lgaz H., Salghi R. - Thiosemicarbazide and thiocarbohydrazide functionalized chitosan as ecofriendly corrosion inhibitors for carbon steel in hydrochloric acid solution, *Int. J. Biol. Macromol.* **107** (2018) 1747-1757. <https://doi.org/10.1016/j.ijbiomac.2017.10.050>
12. Obot I. B., Ankah N. K., Sorour A. A., Gasem Z. M., Haruna K. - 8-Hydroxyquinoline as an alternative green and sustainable acidizing oilfield corrosion inhibitor. *Sustainable Materials and Technologies* **14** (2017) 1-10. <https://doi.org/10.1016/j.susmat.2017.09.001>
13. Mohammadloo H. E., Mirabedini S. M., Pezeshk-Fallah H. - Microencapsulation of quinoline and cerium based inhibitors for smart coating application: Anti-corrosion, morphology and adhesion study, *Prog. Org. Coat.* **137** (2019) 105339. <https://doi.org/10.1016/j.porgcoat.2019.105339>
14. Ivušić F., Lahodny-Šarc O., Čurković H.O., Alar V. - Synergistic inhibition of carbon steel corrosion in seawater by cerium chloride and sodium gluconate, *Corros. Sci.* **98** (2015) 88-97. <https://doi.org/10.1016/j.corsci.2015.05.017>
15. Dastgheib A., Attar M.M., Zarebidaki A. - Evaluation of Corrosion Inhibition of Mild Steel in 3.5 wt% NaCl Solution by Cerium Nitrate. *Met. Mater. Int.* **26** (2019) 1634-1642. <https://doi.org/10.1007/s12540-019-00432-x>
16. Boudellioua H., Hamlaoui Y., Tifouti L., Pedraza F. - Effect of the temperature of cerium nitrate–NaCl solution on corrosion inhibition of mild steel. *Corros. Mater.* **71** (2020) 1300-1309. <https://doi.org/10.1002/maco.201911472>

17. Somers A. E., Hinton B. R. W., de Bruin-Dickason C., Deacon G. B., Junk P. C., Forsyth M. - New, environmentally friendly, rare earth carboxylate corrosion inhibitors for mild steel, *Corros. Sci.* **139** (2018) 430-437. <https://doi.org/10.1016/j.corsci.2018.05.017>
18. Dehghani A., Mostafatabar A. H., Ramezanzadeh B. - Synergistic anticorrosion effect of Brassica Hirta phytoconstituents and cerium ions on mild steel in saline media: Surface and electrochemical evaluations. *Colloids Surf, A Physicochem. Eng. Asp.* **656** (2023) 130503. <https://doi.org/10.1016/j.colsurfa.2022.130503>
19. Liu X., Zhang Y., Pan X., Wang Z. - Rare earth cerium-phenanthroline binary complex as a new corrosion inhibitor for carbon steel in acidic medium, *Res. Chem. Intermed.* **49** (2022) 1235-1257. <https://doi.org/10.1007/s11164-022-04918-z>
20. Hu Y., Cao X., Ma X., Pan J., Cai G., Zhang X., Dong Z. - A bifunctional epoxy coating doped by cerium (III)-8-hydroxyquinoline: Early self-reporting and stimuli-responsive inhibition on corrosion of Al substrate, *Prog. Org. Coat.* **182** (2023) 107616. <https://doi.org/10.1016/j.porgcoat.2023.107616>
21. Dehghani A., Ramezanzadeh B., Poshtiban F., Bahlakeh G. - Construction of a highly-effective/sustainable corrosion protective composite nanofilm based on Aminotris(methylphosphonic acid) and trivalent cerium ions on mild steel against chloride solution, *Constr Build Mater.* **261** (2020) 119838. <https://doi.org/10.1016/j.conbuildmat.2020.119838>
22. Dehghani A., Bahlakeh G., Ramezanzadeh B., Mostafatabar A.H., Ramezanzadeh M. - Estimating the synergistic corrosion inhibition potency of (2-(3,4-)-3,5,7-trihydroxy-4H-chromen-4-one) and trivalent-cerium ions on mild steel in NaCl solution, *Constr Build Mater.* **261** (2020) 119923. <https://doi.org/10.1016/j.conbuildmat.2020.119923>
23. Abd El-Wahab Z.H. - Mixed ligand complexes of nickel(II) and cerium(III) ions with 4-(3-methoxy-4-hydroxybenzylideneamino)-1, 3-dimethyl-2,6-pyrimidine-dione and some nitrogen/oxygen donor ligands, *J. Coord. Chem.* **61** (20) (2008) 3284-3396. <https://doi.org/10.1080/00958970802039996>
24. Liu C., Hou P., Qian B., Hu X. - Smart healable and reportable anticorrosion coating based on halloysite nanotubes carrying 8-hydroxyquinoline on steel, *J. Ind. Eng. Chem.* **118** (2023) 109-118. <https://doi.org/10.1016/j.jiec.2022.10.050>
25. Balaskas A. C., Kartsonakis I. A., Tziveleka L. A., Kordas G. C. - Improvement of anti-corrosive properties of epoxy-coated AA 2024-T3 with TiO₂ nanocontainers loaded with 8-hydroxyquinoline, *Prog. Org. Coat.*, **74** (2012) 418-426. <https://doi.org/10.1016/j.porgcoat.2012.01.005>
26. Spengler E., Fragata F. L., Margarit I. C. P., Mattos O. R. - Corrosion protection of low toxicity paints, *Prog. Org. Coat.* **30** (1997) 51-57. [https://doi.org/10.1016/S0300-9440\(96\)00668-6](https://doi.org/10.1016/S0300-9440(96)00668-6)
27. Le Pen C., Lacabanne C., Pébère N. - Structure of waterborne coatings by electrochemical impedance spectroscopy and a thermostimulated current method: influence of fillers, *Prog. Org. Coat.* **39** (2000) 167-175. [https://doi.org/10.1016/S0300-9440\(00\)00148-X](https://doi.org/10.1016/S0300-9440(00)00148-X)
28. Le Pen C., Lacabanne C., Pébère N. - Characterisation of water-based coatings by electrochemical impedance spectroscopy, *Prog. Org. Coat.* **46** (2003) 77-83. [https://doi.org/10.1016/S0300-9440\(02\)00213-8](https://doi.org/10.1016/S0300-9440(02)00213-8)